JOURNAL OF AIRCRAFT
Vol. 35, No. 4, July–August 1998

Optimized Aeroelastic Couplings for Alleviation of Helicopter Ground Resonance

Farhan Gandhi* and Eric Hathaway†
Pennsylvania State University, University Park, Pennsylvania 16802

Formal optimization methods are used to determine a combination of aeroelastic coupling parameters that can alleviate ground resonance instability of a soft-in-plane rotor. Optimization at a prescribed rotational speed is unable to stabilize ground resonance, as the stability objective function is satisfied merely by moving resonance to a lower rotational speed. A moving-point optimization procedure attempting to stabilize at the rotational speed where damping is a minimum during each optimizer iteration is successful in stabilizing the regressing lag mode at moderate collective pitch. However, these optimal aeroelastic couplings are destabilizing near zero-thrust conditions. A multipoint optimization procedure attempting to stabilize ground resonance simultaneously at low as well as high collective pitch conditions is able to restrict the instability to small values over a broad range of variation in collective pitch and eliminate the destabilizing trend at roll resonance with increasing collective. This configuration could then be stabilized completely by increasing body roll damping. Negative pitch–lag coupling, positive pitch–flap coupling, flap flexibility outboard of pitch, and lag flexibility inboard of pitch were found to be most beneficial.

Introduction

ENSURING adequate aeromechanical stability margins is vital in the design of helicopters with soft-in-plane rotors.[1] Over the years helicopters have been equipped with auxiliary lead–lag dampers to alleviate aeromechanical instability. However, associated with the use of lag dampers are issues such as hub complexity, weight, aerodynamic drag, and maintenance requirements. Additionally, modern-day elastomeric dampers are expensive, susceptible to fatigue, and have complex behavior, including 1) nonlinear amplitude and frequency dependence, 2) blade limit cycle oscillations, and 3) large variations in properties with changes in temperature (including significant loss of damping at extreme temperatures and potential thermal runaway with heat buildup). On account of these factors, a variety of alternatives to auxiliary lag dampers are under consideration.[2,3] The elimination of lag dampers, resulting in the development of a damperless rotor, would further simplify the hub, and reduce weight, aerodynamic drag, and maintenance costs. However, the design of a damperless, yet aeromechanically stable, configuration is truly a challenge, and while several concepts have shown promise, there has been no generally accepted solution for eliminating lag dampers.

One concept for the provision of rotor–body aeromechanical stability is through the use of active controls.[4–8] The use of active controls based on fuselage or rotor state feedback has shown considerable potential and is attractive from an operational and design flexibility standpoint. However, safety and reliability of an active stabilization scheme of highly unstable modes will require careful scrutiny before such an approach can be certified. Of the passive concepts that have been considered, use of aeroelastic couplings to augment rotor–body aeromechanical stability has shown much promise. This subject constitutes the focus of the present paper.

By far the most extensive and noteworthy investigations on the effects of aeroelastic couplings on helicopter aeromechanical stability have been carried out at the U.S. Army Aeroflightdynamics Directorate at NASA Ames Research Center over a period of about two decades. Initially, effects of pitch–lag and flap–lag couplings on the stability of an isolated hingeless rotor in hover were examined,[9–11] and it was shown that a combination of these couplings resulted in a dramatic increase in rotor lag damping. Of even greater interest were the subsequent studies examining the effects of aeroelastic couplings on the coupled rotor–body aeromechanical stability of a hingeless rotor.[12–14] In a landmark study Ormiston[12] analytically examined the effects of pitch–lag and flap–lag couplings on a rotor–body system for both ground resonance and air resonance in hover. It was concluded from this study that aeroelastic couplings are generally not beneficial for ground resonance at zero-blade collective pitch. At higher collective pitch values pitch–lag coupling was found to have a stabilizing effect, but was unable to eliminate ground resonance instability when the body frequency was large. The addition of flap–lag coupling to pitch–lag coupling resulted in some increase in damping in the region of instability. A combination of pitch–lag and flap–lag couplings was very effective in stabilizing air resonance.

Ormiston's analytical study was followed by an experimental investigation of aeromechanical stability characteristics of a model hingeless rotor.[13] It was concluded that for a nonmatched stiffness configuration (typical of most soft-in-plane rotors), the addition of negative pitch–lag coupling, individually as well as in combination with flap–lag coupling, substantially increased lag-regressing mode damping away from resonance conditions. However, modal damping was improved only slightly at rotational speeds where resonance with body pitch and roll modes occurred. For a matched stiffness rotor having a substantially milder instability the addition of negative pitch–lag coupling was able to stabilize the regressing lag mode at resonance. The purpose of this study was to demonstrate that the analytically predicted influence of aeroelastic couplings on aeromechanical stability could indeed be experimentally verified, and not to specifically determine beneficial

Received March 16, 1997; presented as Paper 97-1282 at the AIAA/ASME/ASCE/AHS/ASC 38th Structures, Structural Dynamics, and Materials Conference, Kissimmee, FL, April 7–10, 1997; revision received Nov. 1, 1997; accepted for publication Dec. 17, 1997.

*Assistant Professor, Rotorcraft Center of Excellence, Department of Aerospace Engineering. Member AIAA.
†Graduate Research Assistant, Rotorcraft Center of Excellence, Department of Aerospace Engineering. Student Member AIAA.

or detrimental couplings from an aeromechanical stability standpoint.

Other researchers have shown that negative pitch–lag coupling stabilizes air resonance, while pitch–flap and flap–lag couplings are relatively uninfluential.[15–17] In Ref. 18 it was observed that the extent of the influence of pitch–lag coupling in improving aeromechanical stability in hover was dependent on parameters such as blade lag frequency and hub–fuselage vertical offset. Further, values of pitch–lag coupling beneficial for hover, in general, were detrimental for ground resonance stability. In an attempt to alleviate aeromechanical instabilities of the model rotor tested in Ref. 13, Venkatesan[19] analytically examined the individual as well as combined effects of pitch–lag, pitch–flap, and structural flap–lag couplings. For the nonmatched stiffness configuration Venkatesan verified earlier observations, that pitch–lag and flap–lag couplings were not particularly beneficial at resonance conditions with body pitch and roll. It was observed, however, that positive pitch–flap coupling increased the damping at resonance conditions. By a suitable combination of structural flap–lag, negative pitch–lag, and positive pitch–flap couplings, the lag-regressing mode could be stabilized over the whole range of rotational speeds. However, this was done only at a single value of collective pitch.

Clearly, aeroelastic couplings have shown the potential of increasing regressing lag mode damping and improving coupled rotor–body aeromechanical stability. This leads to the question whether it would be generally possible to exploit aeroelastic couplings in the design of aeromechanically stable helicopters free of auxiliary lag dampers. The real challenge in designing a damperless rotor lies in determining an optimum combination of aeroelastic couplings that results in satisfactory rotor–body aeromechanical stability characteristics over a broad range of variations in configuration and operating conditions. The literature indicates that while a certain aeroelastic coupling parameter may have a stabilizing influence over a range of operating conditions, it may be ineffective or destabilizing in other conditions. For example, negative pitch–lag coupling is reported to be beneficial for stabilizing air resonance, but not for alleviating ground resonance. Aeroelastic couplings that stabilize resonance with body roll may have a destabilizing influence at resonance with body pitch, particularly for matched stiffness rotors.[19] If auxiliary lag dampers are to be eliminated, the aeroelastic couplings should provide adequate stability at various rotational speeds, thrust levels, for variations in body inertia, and at different operating conditions (such as ground contact and airborne conditions). Of the different operating conditions the literature indicates that the ground contact condition is the most difficult to stabilize.

The present study attempts to determine a combination of aeroelastic couplings that can stabilize ground resonance of a soft-in-plane rotor, over its spectrum of rotational speeds, at various thrust levels, and for variations in body frequencies. Such a task has not been attempted in any of the previous studies, most of which have parametrically examined aeromechanical stability trends, at a single thrust level, as a result of a few selected values of aeroelastic coupling parameters. The present study treats the aeroelastic couplings as continuous variables and uses formal design optimization in an attempt to determine a combination of couplings that completely stabilizes ground resonance. The study provides considerable insight into the subtleties involved in the definition and formulation of the design-optimization problem, and addresses the resolution of the conflicting demands at low- and high-thrust conditions. Further, the influence of the optimized couplings are examined at off-design conditions. The present study does not focus on implementation methods for the aeroelastic couplings, but is restricted to establishing the required couplings that will stabilize ground resonance and potentially allow the elimination of auxiliary lag dampers.

Rotor–Fuselage Analytical Model

In the analytical model used in the present study the rotor blades are assumed to be rigid, have uniform mass density, and undergo flap rotations β and lag rotations ζ about spring-restrained offset hinges. The blade root flap and lag stiffnesses, along with the hinge offsets, determine the flap and lag frequencies. The aerodynamic loads on the rotor blades are calculated using quasisteady strip theory, assuming a uniform inflow. The fuselage or pylon is assumed to undergo rigid body pitch and roll rotations (α_x and α_y) about its c.m. (located at a distance h directly below the rotor hub). The required fuselage physical properties are the pitch and roll inertia along with the stiffness and damping in pitch and roll rotations. The rotor–fuselage equations of motion are linearized about the equilibrium (trim) condition to obtain the perturbation equations. The perturbation flap and lag equations for the individual blades are transformed to the nonrotating coordinate system using multiblade coordinate transformation. For a three-bladed rotor this transformation yields a collective and two cyclic flap and lag equations in the nonrotating coordinate system. However, only the cyclic flap and lag equations need to be retained. The collective flap and lag equations do not couple with the fuselage motions and, hence, can be deleted from the aeromechanical stability analytical model. Thus, the rotor–fuselage model has six degrees of freedom: cyclic flap (β_{1c} and β_{1s}), cyclic lag (ζ_{1c} and ζ_{1s}), and fuselage roll and pitch (α_x and α_y). In the nonrotating frame the resulting constant coefficient system can be represented in the following form:

$$[M]\{\ddot{\boldsymbol{q}}\} + [C]\{\dot{\boldsymbol{q}}\} + [K]\{\boldsymbol{q}\} = \{\mathbf{0}\} \tag{1}$$

where $[M]$, $[C]$, and are $[K]$ are the 6×6 mass, damping, and stiffness matrices, respectively, and

$$\{\boldsymbol{q}\} = \lfloor \beta_{1c}\beta_{1s}\zeta_{1c}\zeta_{1s}\alpha_x\alpha_y \rfloor^T \tag{1a}$$

The eigenvalues of Eq. (1) yield the modal frequencies and decay rates.

The aeroelastic coupling parameters considered [and contained in Eq. (1)] are pitch–flap coupling $K_{P\beta}$, pitch–lag coupling $K_{P\zeta}$, and the flap–lag coupling parameters R_β and R_ζ. The pitch–flap and pitch–lag couplings result in variations in blade pitch θ as a result of perturbation flap and lag motions. Thus

$$\theta = -K_{P\beta}\beta - K_{P\zeta}\zeta \tag{2}$$

Structural flap–lag coupling is a result of blade flap and lag flexibility outboard of the pitch bearing. In Ref. 20 flap–lag coupling was modeled using orthogonal hub flap and lag springs $k_{\beta H}$ and $k_{\zeta H}$, respectively, inboard of the pitch bearing; and orthogonal blade flap and lag springs $k_{\beta B}$ and $k_{\zeta B}$, respectively, outboard of the pitch bearing. Based on this system of springs, effective flap and lag flexural stiffnesses k_β and k_ζ were defined as

$$k_\beta = \frac{k_{\beta H}k_{\beta B}}{k_{\beta H} + k_{\beta B}} \quad \text{and} \quad k_\zeta = \frac{k_{\zeta H}k_{\zeta B}}{k_{\zeta H} + k_{\zeta B}} \tag{3}$$

Structural flap–lag coupling parameters are then defined as

$$R_\beta = k_\beta / k_{\beta B} \quad \text{and} \quad R_\zeta = k_\zeta / k_{\zeta B} \tag{4}$$

with $R_\beta = 1$, meaning the flap flexibility is entirely outboard of the pitch bearing with the hub being rigid in flap, and $R_\beta = 0$, meaning the flap flexiblity is entirely in the hub with the region outboard of the pitch bearing being rigid in flap. Similar interpretations about the lag flexibility being outboard or inboard of the pitch bearing can be made for $R_\zeta = 1$ or 0, respectively. In general, if there is some flexibility in both the hub and the blade, R_β and R_ζ assume values between 0 and 1.

It should be noted that most of the previous studies that examined the influence of aeroelastic couplings on aeromechanical stability characteristics assumed that $R_\beta = R_\zeta$, implying that the percentages of flexibility outboard and inboard of the pitch bearing were identical for flap and lag. In the present study, however, R_β and R_ζ are allowed to assume different values. The elastic restoring moments in flap and lag are then written as

$$\begin{Bmatrix} M_\beta \\ M_\zeta \end{Bmatrix} = \begin{bmatrix} \bar{K}_{\beta\beta} & \bar{K}_{\beta\zeta} \\ \bar{K}_{\beta\zeta} & \bar{K}_{\zeta\zeta} \end{bmatrix} \begin{Bmatrix} \beta \\ \zeta \end{Bmatrix} \tag{5}$$

where

$$\bar{K}_{\beta\beta} = (1/\Delta)[k_\beta + (R_\beta k_\zeta - R_\zeta k_\beta)\sin^2\bar{\theta}]$$

$$\bar{K}_{\zeta\zeta} = (1/\Delta)[k_\zeta - (R_\beta k_\zeta - R_\zeta k_\beta)\sin^2\bar{\theta}]$$

$$\bar{K}_{\beta\zeta} = (1/\Delta)[-(R_\beta k_\zeta - R_\zeta k_\beta)\cos\bar{\theta}\,\sin\bar{\theta}] \tag{6}$$

$$\Delta = 1 + (2R_\beta R_\zeta - R_\beta - R_\zeta)\sin^2\bar{\theta} + [R_\zeta(1 - R_\zeta)(k_\beta/k_\zeta) + R_\beta(1 - R_\beta)(k_\zeta/k_\beta)]\sin^2\bar{\theta}$$

In Eq. (6), $\bar{\theta}$ denotes the blade pitch.

Validation of Analytical Model

The analytical model is validated using experimental results in Ref. 13. Rotor–fuselage properties for this configuration are as follows: number of blades = 3; radius = 81.1 cm; chord = 4.19 cm; hinge offset = 8.51 cm; lock number = 7.37; blade profile = NACA 23012; drag coefficients c_{d0} and c_{d2} = 0.0079 and 1.7, respectively; pitching moment coefficient c_m = −0.012; lift-curve slope a = 5.73; lift coefficient at zero angle of attack = 0.15; nonrotating flap frequency $\omega_{\beta o}$ = 3.13 Hz; nonrotating lag frequency $\omega_{\zeta o}$ = 6.70 Hz; body roll frequency ω_x = 4 Hz; body pitch frequency ω_y = 2 Hz; lag damping η_ζ = 0.52%; body roll damping η_x = 0.929%; body pitch damping η_y = 3.20%; roll inertia = 183.0 gm-m^2; pitch inertia = 633.0 gm-m^2; and blade inertia = 17.3 gm-m^2. Figure 1 shows the variation in regressing lag damping vs rotational speed, for 0-deg collective. It is seen that the analytically predicted results compare very well with experiment (depicted by symbols). It should be noted that for the analytical results in Fig. 1 unsteady aerodynamic effects were included through the use of a dynamic inflow model.[21] Thus, the system state vector had inflow states in addition to the rotor–fuselage states. Figures 2 and 3 show the variation of regressing lag damping vs rotational speed at 9-deg collective, for the cases of no aeroelastic coupling and for a pitch–lag coupling $K_{P\zeta}$ = −0.4, respectively. Once again, in both cases, the analytical predictions compare well with experimental results. Finally, Fig. 4 shows a variation of regressing lag damping vs collective pitch at rotational speeds of 760 and 820 rpm. Again, the analytical results compare very well with the experiment.

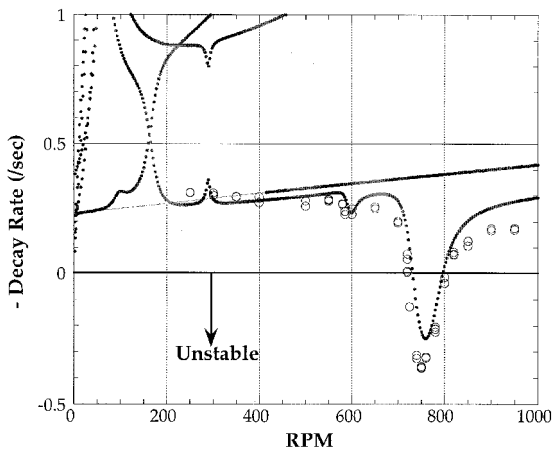

Fig. 1 Variation of regressing lag damping vs rotational speed at 0-deg collective.

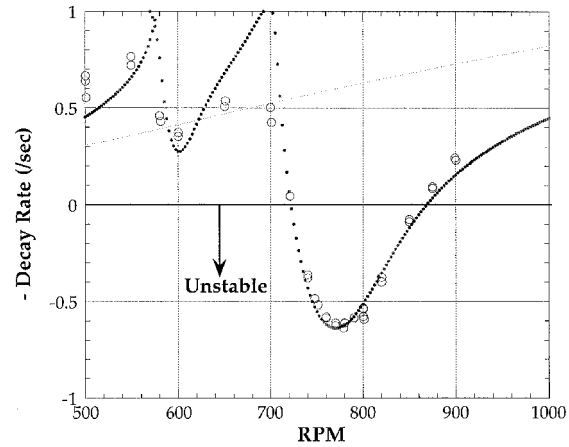

Fig. 2 Variation of regressing lag damping vs rotational speed at 9-deg collective.

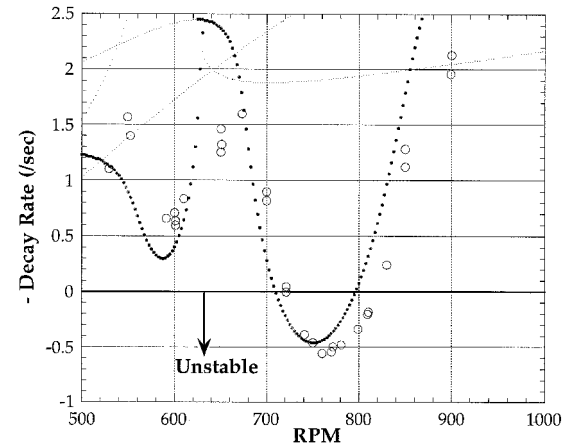

Fig. 3 Variation of regressing lag damping vs rotational speed at 9-deg collective ($K_{P\zeta}$ = −0.4).

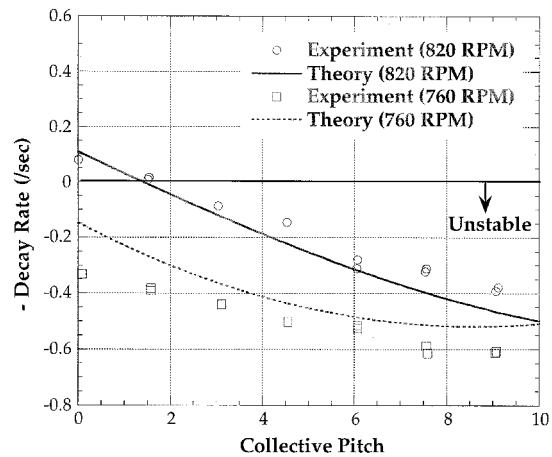

Fig. 4 Variation of regressing lag damping vs collective at 760 and 820 rpm.

For subsequent parametric study and optimization results dynamic inflow effects are neglected in the interest of simplicity. This is done by taking into consideration the following factors:

1) Dynamic inflow has a significant influence on body mode damping but a much smaller influence on regressing lag mode damping, and it is the latter that is the focus of the present study.

2) At moderate to high-thrust conditions the influence of dynamic inflow on regressing lag damping will further diminish.

Influence of Individual Aeroelastic Couplings on Ground Resonance

Before invoking design optimization methods the influence of individual aeroelastic couplings on ground resonance is examined at a moderate collective pitch of 5 deg, for the configuration described in the preceding section.

Pitch–Lag Coupling

Figure 5 shows the influence of negative pitch–lag coupling on lag damping in ground resonance. It is seen that while there is no change in the minimum damping values at resonance, negative pitch–lag coupling increases the damping away from resonance. The net effect is that the range of rotational speeds over which instability is encountered is significantly reduced.

Pitch–Flap Coupling

In Fig. 6 it is seen that positive pitch–flap coupling is able to increase the minimum damping at resonance conditions. The results indicate that after obtaining a significant increase in damping for small values of pitch–flap coupling, further increases in pitch–flap coupling result in smaller additional increases in minimum damping.

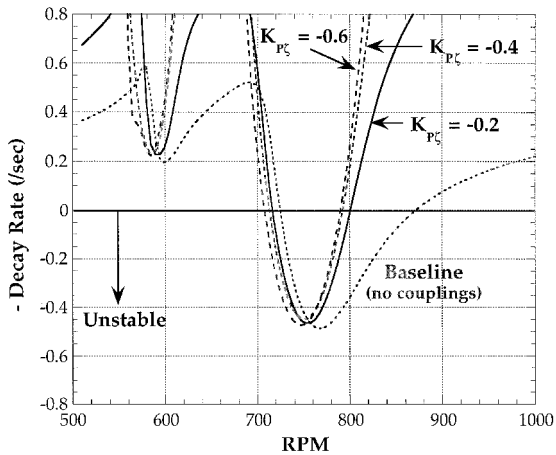

Fig. 5 Influence of pitch–lag coupling on lag damping in ground resonance (5-deg collective).

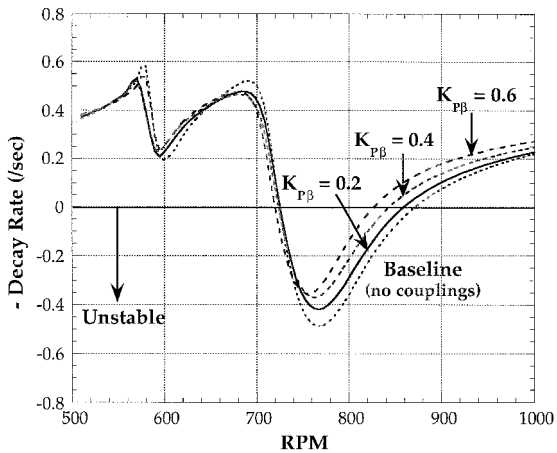

Fig. 6 Influence of pitch–flap coupling on lag damping in ground resonance (5-deg collective).

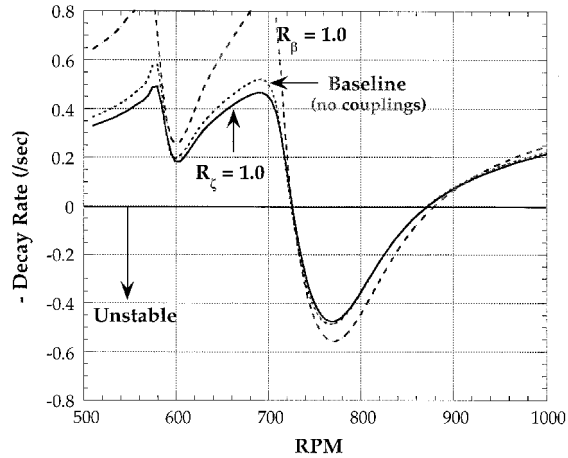

Fig. 7 Influence of flap–lag coupling on lag damping in ground resonance (5-deg collective).

In Figs. 5 and 6 it is seen that both negative pitch–lag coupling as well as positive pitch–flap coupling tend to shift the resonance condition to a slightly lower rotational speed.

Structural Flap–Lag Coupling

Figure 7 shows that structural flap–lag couplings are unable to increase the minimum damping at roll resonance. Of the two parameters lag damping is more sensitive to changes in R_β. The damping with $R_\zeta = 1$ is almost identical to the baseline. For the case $R_\beta = R_\zeta = 1$ (results not shown in Fig. 7), the regressing lag damping was found to be almost identical to the case $R_\beta = 1$ ($R_\zeta = 0$). It should be mentioned that flap–lag coupling is likely to have larger influences at higher values of collective.

Determination of Aeroelastic Couplings Through Design Optimization

In this section formal optimization is used in an attempt to alleviate ground resonance instability of the configuration shown in the preceding text. Pitch–flap coupling $K_{P\beta}$, pitch–lag coupling $K_{P\zeta}$, and the flap–lag coupling parameters R_β and R_ζ are treated as the design variables. Optimization is carried out with appropriate constraints using the International Mathematical and Statistical Library subroutines.

Single-Point Optimization

Design optimization is initially carried out at a moderate thrust condition (collective pitch of 5 deg). Because the baseline system (without any aeroelastic couplings) has a minimum damping at about 770 rpm, the objective function to be minimized is defined as follows:

$$F(D_j) = (\sigma_{770} - \bar{\sigma}_{770})^2 \tag{7}$$

where σ_{770} denotes the regressing lag mode decay rate at 770 rpm; $\bar{\sigma}_{770}$ denotes the desired regressing lag decay rate at 770 rpm (which was set at -0.1/s, stable); and D_j denotes the jth design variable.

The following constraints are imposed on the design variables:

$$-1 \le K_{P\beta} \le 1, \quad -1 \le K_{P\zeta} \le 1, \quad 0 \le R_\beta \le 1, \quad 0 \le R_\zeta \le 1 \tag{8}$$

The sensitivity gradients, $\partial\sigma_{770}/\partial D_j$, required in the optimization procedure, are calculated numerically by perturbing the individual design variables. The optimization procedure yielded the following results:

$$K_{P\beta} = 0.328, \quad K_{P\zeta} = -0.448, \quad R_\beta = 0.997, \quad R_\zeta = 0.998 \tag{9}$$

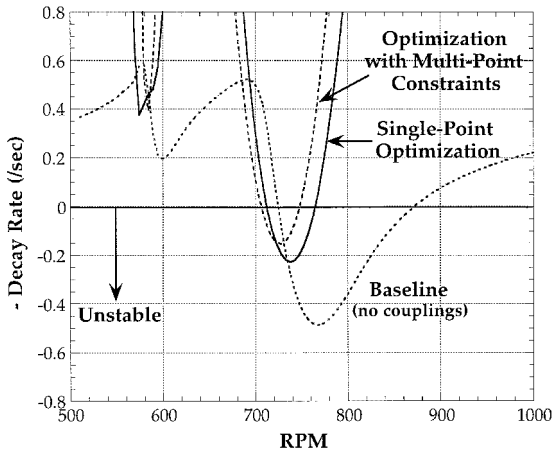

Fig. 8 Influence of couplings obtained using single-point optimization and single-point optimization with multipoint constraints on regressing lag damping in ground resonance (5-deg collective).

Figure 8 shows the variation of regressing lag damping vs rotational speed when these optimal values of aeroelastic couplings are used. It is interesting to note that satisfaction of the objective function ($\sigma_{770} = \bar{\sigma}_{770}$) is accomplished by moving the resonance condition to a lower rotational speed. The net result is that an increase in regressing lag damping is obtained over the baseline but that instability of the regressing lag mode is still present. Similar results were obtained for increasing values of $\bar{\sigma}_{770}$, i.e, resonance moved to a lower rotational speed and instability persisted.

Of the optimized aeroelastic coupling parameters, the structural flap–lag couplings did not have a major influence. The initial guess for R_β and R_ζ was 1, and the optimized values remained close to the initial guess. When the initial guess was selected at 0, the optimizer yielded virtually the same values of $K_{P\beta}$ and $K_{P\zeta}$, but the values R_β and R_ζ remained close to 0. Even in the latter case (R_β, $R_\zeta \approx 0$), the aeromechanical stability characteristics were very similar to the single-point optimization results presented in Fig. 8.

Single-Point Optimization with Multipoint Constraints

It was seen that the single-point optimization procedure was effective in producing the desired level of damping at the specified rotational speed (770 rpm), but this was achieved only by moving the resonance condition to another rotational speed. To improve aeromechanical stability over a wide range of rotational speeds and to prevent satisfaction of the objective function merely by moving the resonance to a different rotational speed, stability constraints are introduced at a number of rotational speeds. The objective function minimized

$$F(D_j) = (\sigma_{775} - \bar{\sigma}_{775})^2 \tag{10}$$

is similar to Eq. (7), but inequality constraints

$$\begin{aligned} g_1(D_j) &= \sigma_{725} \le 0, \qquad g_2(D_j) = \sigma_{750} \le 0 \\ g_3(D_j) &= \sigma_{800} \le 0, \qquad g_4(D_j) = \sigma_{825} \le 0 \end{aligned} \tag{11}$$

are introduced in addition to constraints on the design variables [Eq. (8)].

This problem requires the design variables to be perturbed at each of the rotational speeds considered, to calculate sensitivity gradients $\partial\sigma_{725}/\partial D_j$, $\partial\sigma_{750}/\partial D_j$, $\partial\sigma_{775}/\partial D_j$, $\partial\sigma_{800}/\partial D_j$, and $\partial\sigma_{825}/\partial D_j$ in each optimizer iteration.

The present optimization procedure yielded the following results (at 5-deg collective pitch):

$$K_{P\beta} = 0.622, \quad K_{P\zeta} = -0.641, \quad R_\beta = 0.983, \quad R_\zeta = 1.0 \tag{12}$$

Regressing lag damping characteristics with these aeroelastic coupling parameters are superposed on Fig. 8. The level of instability as well as the range of rotational speeds over which instability is present are both reduced as compared to the single-point optimization results. However, the system is not completely stabilized and the inequality constraint g_1 [Eq. (11)] is violated.

Moving-Point Optimization

To completely eliminate the possibility that an objective function at a prescribed rotational speed is satisfied by moving the resonance to a different rotational speed, a moving-point optimization procedure is formulated. The objective function to be minimized is

$$F(D_j) = (\sigma_{\min} - \bar{\sigma}_{\min})^2 \tag{13}$$

subject to constraints on the design variables [Eq. (8)]. In this objective function, $\sigma_{\min}$ denotes the minimum decay rate (which occurs at different rotational speeds as the values of aeroelastic coupling parameters change during the course of the optimization process), and $\bar{\sigma}_{\min}$ denotes the desired minimum decay rate (which was set at -0.1/s, stable). In this procedure, during each iteration in the optimization process, the rotational speed at which the damping is a minimum is determined and the optimizer then seeks to stabilize the regressing lag mode at this rotational speed. Thus, there is no possibility that an objective function at a prescribed rotational speed will be satisfied by moving the resonance to another rotational speed.

The moving-point optimization procedure yielded the following results (at 5-deg collective)

$$K_{P\beta} \approx 0.6, \quad K_{P\zeta} = -1.0, \quad R_\beta = 1.0, \quad R_\zeta = 0.0 \tag{14}$$

It is interesting to note that the value of R_ζ has changed from 1.0, in previous optimization efforts, to 0 in this case. A possible explanation for this may have to do with $K_{P\zeta}$ having reached the constraint, -1.0. The optimizer may now be working with less sensitive parameters like R_ζ, in an attempt to satisfy the objective function. Figure 9 shows the variation of regressing lag damping vs rotational speed when these optimal values of aeroelastic couplings are used. It is seen that this configuration stabilizes the regressing lag mode over the entire range of rotational speeds.

Because large values of pitch–flap coupling may have some other undesirable effects (for example, on handling qualities), optimization was repeated using the constraint $-0.4 \le K_{P\beta} \le 0.4$ (in place of $-1 \le K_{P\beta} \le 1$). The optimal aeroelastic couplings in this case were

$$K_{P\beta} = 0.4, \quad K_{P\zeta} = -1.0, \quad R_\beta = 1.0, \quad R_\zeta = 0.0 \tag{15}$$

However, it is seen in Fig. 9 that the influence of the reduced pitch–flap coupling (from $K_{P\beta} = 0.6$ to $K_{P\beta} = 0.4$) on regressing

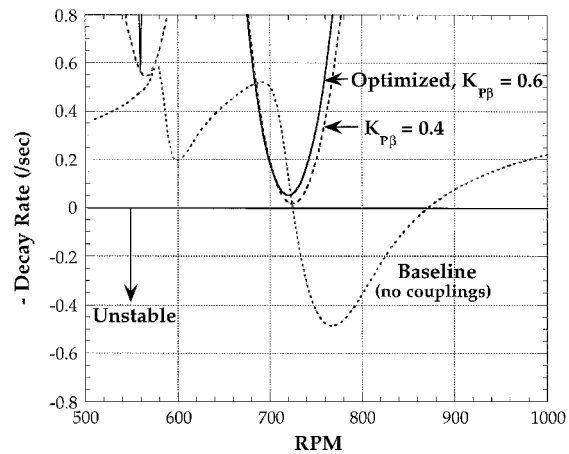

Fig. 9 Influence of couplings obtained using moving-point optimization on lag damping in ground resonance (5-deg collective).

lag mode damping is not very significant. This is consistent with the earlier observation that increments in $K_{P\beta}$ beyond a moderate value result in relatively small changes in aeromechanical stability characteristics (Fig. 6).

Next, the influence of these optimal couplings (determined through a moving-point optimization procedure at 5-deg collective) must be examined at different blade pitch settings. Figure 10 shows the variation of regressing lag damping vs rotational speed at 0-deg collective pitch, obtained using the optimized aeroelastic couplings in Eq. (14). It is seen that optimal couplings at 5-deg collective seriously degrade the stability at 0-deg collective (as compared to the baseline with no aeroelastic couplings). Examination of similar plots (regressing lag damping vs rotational speed) at different values of collective pitch showed that the aeroelastic couplings obtained through moving-point optimization at 5 deg [Eq. (14)] are stabilizing at moderate-to-high collective pitch settings, but are destabilizing for low collective pitch settings close to 0 deg.

A moving-point optimization carried out at 0-deg collective pitch yielded the following optimal aeroelastic couplings:

$$K_{P\beta} = -1.0, \quad K_{P\zeta} = 0.07226, \quad R_\beta = 0.0, \quad R_\zeta = 0.0 \qquad (16)$$

It is seen in Fig. 11 that while the preceding couplings eliminate aeromechanical instability at 0-deg collective, they are very strongly destabilizing at increasing collective pitch values.

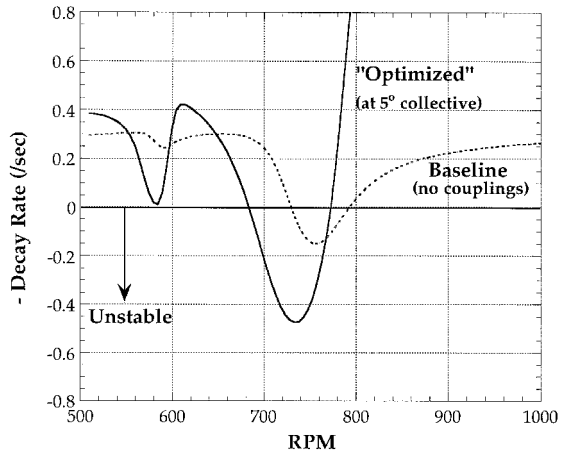

Fig. 10 Influence of couplings obtained using moving-point optimization at 5-deg collective, on lag damping in ground resonance at 0-deg collective.

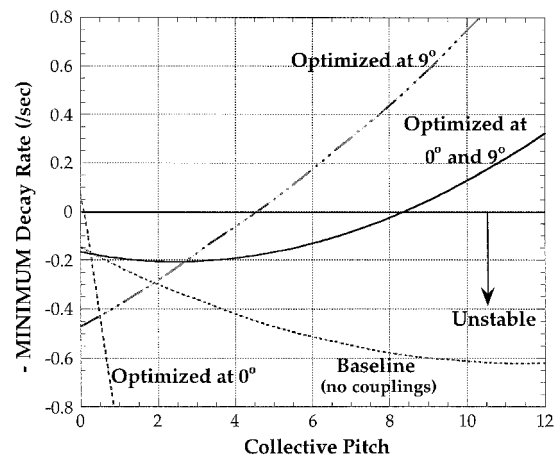

Fig. 11 Variation of minimum damping vs collective pitch using different optimization schemes.

A moving-point optimization carried out at 9-deg collective pitch yielded the following optimal aeroelastic couplings:

$$K_{P\beta} = 0.6288, \quad K_{P\zeta} = -1.0, \quad R_\beta = 1.0, \quad R_\zeta = 0.0 \qquad (17)$$

Figure 11 shows that these couplings result in very large stability margins at high collective pitch values, but the damping decreases with decreasing collective. Eventually, the regressing lag mode becomes unstable at $\theta_o < 5$ deg, and for $\theta_o < 2$ deg the damping in the regressing lag mode falls to values lower than the baseline configuration (no aeroelastic couplings).

It should be noted that the optimal aeroelastic couplings at 0-deg collective [Eq. (16)] are fundamentally different from the optimal couplings for moderate or high collective pitch [Eqs. (14) and (17)].

Multipoint Optimization at 0 and 9 Deg

In an attempt to stabilize ground resonance over a wide range of variation in collective pitch the previously described moving-point optimization procedure is simultaneously implemented at two different collective pitch settings, 0 and 9 deg. The objective function to be minimized is

$$F(D_j) = W_{0\,\mathrm{deg}}(\sigma_{\min}^{0\,\mathrm{deg}} - \bar{\sigma}_{\min}^{0\,\mathrm{deg}})^2 + W_{9\,\mathrm{deg}}(\sigma_{\min}^{9\,\mathrm{deg}} - \bar{\sigma}_{\min}^{9\,\mathrm{deg}})^2 \qquad (18)$$

subject to constraints on design variables [Eq. (8)].

The optimization procedure yielded the following results:

$$K_{P\beta} = 0.814, \quad K_{P\zeta} = -0.221, \quad R_\beta = 1.0, \quad R_\zeta = 0.0 \qquad (19)$$

Figure 11 indicates that while these aeroelastic couplings obtained through simultaneous optimization at 0 and 9 deg are unable to completely stabilize the regressing lag mode, the level of instability is restricted to a fairly modest value over a broad range of variation in collective pitch and the destabilizing trend with increasing collective pitch seen in the baseline configuration is alleviated. It is also seen that over the entire collective pitch range the damping in the regressing lag mode is about as much as or greater than the baseline. Up to a collective pitch of 5 deg the minimum damping in the regressing lag mode remains fairly uniform and then starts slowly increasing with the collective.

Attempts to further increase the minimum damping at low to moderate values of collective pitch by varying the weights $W_{0\,\mathrm{deg}}$ and $W_{9\,\mathrm{deg}}$ were unsuccessful. Even though it appears in Fig. 11 that it should be possible to trade stability margin at high-thrust conditions for increased damping at lower collective pitch, the aeroelastic coupling requirements are such that large decreases in stability at high collective resulted in only very small increases in stability at low collective. Similarly, no significant improvement in minimum lag damping was obtained for optimization at a different set of collective pitch values. For example, when multipoint optimization was carried out simultaneously at 0 and 5 deg, the results were qualitatively similar to those obtained by optimizing at 0 and 9 deg.

It is interesting to note that the optimal couplings [Eq. (19)] yield $R_\beta = 1$ and $R_\zeta = 0$. This suggests that the flap flexibility should be outboard of the pitch bearing, whereas the lag flexibility should be inboard of the pitch bearing for best aeromechanical stability characteristics in ground resonance. However, if R_β and R_ζ are constrained to be equal, the following results are obtained:

$$K_{P\beta} = 0.7729, \quad K_{P\zeta} = -0.2705, \quad R_\beta = 1.0, \quad R_\zeta = 1.0 \qquad (20)$$

This confirms the earlier observation that R_β is the more dominant of the flap–lag coupling parameters.

If R_β and R_ζ are both constrained to be zero, the following optimal results are obtained:

$$K_{P\beta} = 0.7430, \quad K_{P\zeta} = -0.3319, \quad R_\beta = 0.0, \quad R_\zeta = 0.0 \qquad (21)$$

Figure 12 shows the variation of regressing lag damping at 5-deg collective for three cases: 1) no secondary constraints on R_β, R_ζ, i.e, $0 \le R_\beta \le 1$, $0 \le R_\zeta \le 1$; 2) $R_\beta = R_\zeta = R$ ($0 \le R \le 1$); and 3) $R_\beta = R_\zeta = 0$. The minimum damping for $R_\beta = R_\zeta$ (case 2) is very close to that obtained in case 1. However, for $R_\beta = R_\zeta = 0$ (case 3), some decrease in minimum damping is observed. Thus, if R_β and R_ζ are constrained to be equal (as was done in previous studies), it is more effective to shift the lag flexibility outboard of the pitch bearing than it is to bring the flap flexibility inboard.

From Fig. 11 it appears that one of three potential design strategies can be adopted: 1) stabilize ground resonance at 0-deg collective, sharply destabilizing it at nonzero collective; 2) stabilize ground resonance at higher collectives, destabilizing it at 0-deg collective; or 3) keep the level of instability small over a wide range of collective pitch values.

Of the strategies just suggested, accepting a mild instability over a wide range of collective pitch values appears to be the most attractive. In such a case it may be possible to eliminate auxiliary lead–lag dampers by using high-damping flexures or other techniques such as constrained layer damping treatments. Another possibility could be to alleviate the mild instability by increasing the damping in the landing gears. For the results presented thus far, damping ratios in the fuselage pitch and roll mode were, respectively, 3.20 and 0.929%. Figure 13 shows that if the roll damping is increased to about 9%, instability can be alleviated for all values of collective pitch. This level of roll damping is typical for helicopters with oleos attached to the landing-gear struts. Alternatively, a design strategy can be adopted whereby optimal aeroelastic couplings that are stabilizing over certain conditions are introduced, with the understanding that instabilities at other conditions would have to be stabilized by some other means. For example, if aeroelastic couplings that were stabilizing at moderate-to-high thrust were introduced, active controls could be used to stabilize flat pitch operations.

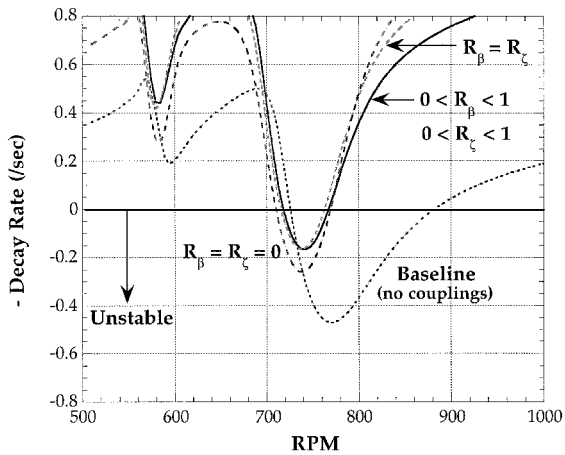

Fig. 12 Influence of flap–lag coupling parameters on aeromechanical stability characteristics at 5-deg collective.

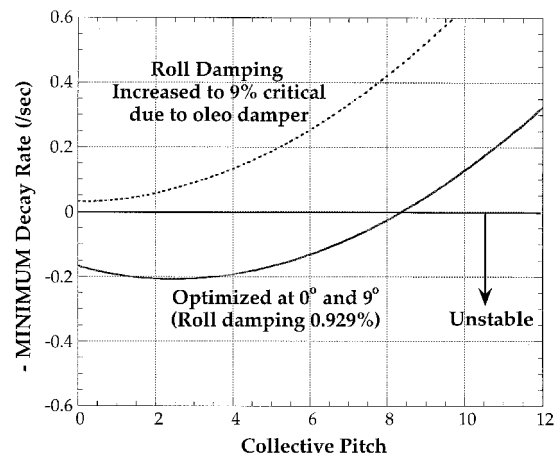

Fig. 13 Regressing lag mode stabilized by increasing roll damping.

Variation in Body Frequencies

The effectiveness of optimized aeroelastic couplings at off-design conditions is examined by allowing up to ±25% variation in body inertias. Such variations are common during operation and have the effect of changing the body frequencies. Figure 14 shows the variation of minimum damping vs body-roll inertia at 5-deg collective. It is seen that for both the baseline configuration (no aeroelastic couplings) as well as for a configuration with optimal aeroelastic couplings [Eq. (14)], a decrease in roll inertia results in lower damping. Thus, in the design of a damperless helicopter it is important to ensure that the optimal aeroelastic couplings provide aeromechanical stability not just at the baseline inertia, but also at the minimum possible value of roll inertia (generally associated with zero payload). Figure 14 indicates that if optimal aeroelastic couplings are able to alleviate instability at the lowest possible value of roll inertia, these couplings would provide more than adequate stability margins for increased values of roll inertia.

A moving-point optimization procedure at 5-deg collective, but at −25% of the baseline roll inertia, yielded the following aeroelastic couplings:

$$K_{P\beta} = 0.75, \quad K_{P\zeta} = -1.0, \quad R_\beta = 1.0, \quad R_\zeta = 0.0 \qquad (22)$$

Minimum damping values obtained using these couplings are superposed on Fig. 14. No significant alleviation in the destabilizing trend with decreasing inertia was obtained by optimizing at the most critical point.

A ±25% variation in pitch inertia results in a variation in the minimum damping at the pitch resonance. However, because damping at pitch resonance in all cases remains much greater than the damping at roll resonance, this does not constitute a critical condition.

Reduction in roll inertia increases the roll frequency. An increase in landing gear effective stiffness in roll would have a similar influence of increasing the roll frequency and destabilizing both the baseline configuration as well as the optimized configuration. However, the damping in the optimized configuration would again be higher and any instability would be weaker.

Although parameters such as blade flap or lag frequencies could influence some of the observations made so far, unlike thrust level, body inertia, and rotational speed, these param-

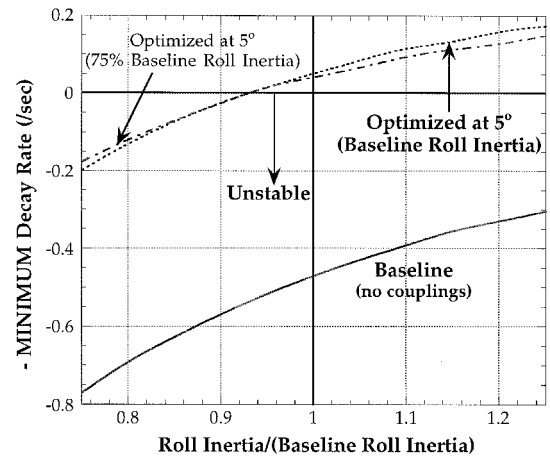

Fig. 14 Variation of minimum lag damping vs roll inertia at 5-deg collective.

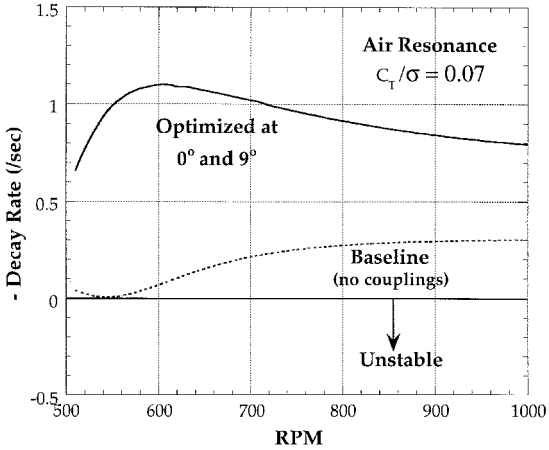

Fig. 15 Influence of couplings (obtained through multipoint optimization on ground at 0 deg and 9 deg) on air resonance in hover.

eters are not anticipated to undergo variations during operation and are thus not considered.

Air Resonance

Influence of the optimal aeroelastic couplings on hover air resonance is briefly examined. In the present study this is done by setting the body pitch and roll frequencies to zero. It should be noted that the pitch and roll springs in the baseline configuration were quite soft and may not be accurately representative of ground resonance of a helicopter, but more so of a condition between ground and air resonance. Figure 15 shows the regressing lag damping in hover (body frequencies set to zero) using couplings obtained through multipoint optimization on ground at 0 and 9 deg [Eq. (19)]. The baseline configuration was marginally stable in air and was further stabilized by the optimal couplings in Eq. (19). It should be noted that the damping levels at different rotational speeds in Fig. 15 do not correspond to a single value of collective pitch. Rather the rotor is trimmed to a constant thrust (corresponding to a nominal C_T/σ of 0.07 at 720 rpm) to enable the vehicle to remain airborne.

Summary and Concluding Remarks

1) From the parametric studies on the effects of individual aeroelastic couplings on ground resonance stability characteristics at a moderate collective pitch of 5 deg, the following conclusions are drawn: Positive pitch–flap coupling is able to increase the minimum damping at resonance. Small-to-moderate values of pitch–flap coupling are adequate in increasing the minimum damping. Additional increase in lag damping by further increasing pitch–flap coupling is generally small. With negative pitch–lag coupling there is no increase in minimum damping at resonance, but there is a significant increase in damping away from resonance. This results in a decrease in the range of rotational speeds over which instability is present. Structural flap–lag coupling does not, individually, yield any benefit.

2) In using single-point optimization at a specified rotational speed, the aeromechanical stability objective function is satisfied merely by moving the resonance instability to a different rotational speed. The introduction of additional stability constraints at multiple rotational speeds provides some improvement but does not eliminate instability.

3) A moving-point optimization procedure yields aeroelastic coupling parameters that stabilize ground resonance at a given collective pitch. However, the optimal couplings at moderate or high-pitch conditions are destabilizing at 0-deg collective and vice versa.

4) Using multipoint optimization, involving simultaneous stabilization at two different collective pitch settings (typically flat pitch and moderate-to-high collective pitch), it was possible to weaken the instability over the range of collective pitch values and alleviate the destabilizing trend with increasing values of collective. Subsequently, by increasing roll damping to about 9% critical, it was possible to eliminate instabilities at all values of collective pitch.

5) Of the two flap–lag coupling parameters, R_β and R_ζ, the largest increase in minimum damping is obtained, in general, when R_β is close to unity and R_ζ is close to zero. This implies that the flap flexibility should be outboard of pitch, whereas lag flexibility should be inboard (in addition to negative pitch–lag coupling and positive pitch–flap coupling). Of the two parameters, R_β has a larger influence. Thus, if the two must be constrained to be equal, it is advantageous to have both flap and lag flexibility outboard.

6) The destabilizing trend with reduction in roll inertia (seen in the baseline configuration) persists in configurations with optimal aeroelastic couplings. However, if the optimized configuration has an instability at the lowest roll inertia it is much weaker than that of the baseline.

7) By choosing the correct optimal combination of aeroelastic couplings, significant improvement in aeromechanical stability characteristics was obtained over a range of conditions (such as various rotational speeds, thrust levels, and changes in body inertia). Complete stabilization could be achieved for the present configuration only after significantly increasing the body roll damping. However, it is not a general conclusion that such a large increase in roll damping would be necessary to stabilize any configuration.

8) The aeroelastic couplings obtained through multipoint optimization on ground at 0 and 9 deg were stabilizing in hover.

Acknowledgments

This research was supported by the U.S. Army Research Office under Contract DAAG55-97-1-0347, with Gary L. Anderson as Technical Monitor. The first author would like to acknowledge Robert A. Ormiston, U.S. Army Aeroflightdynamics Directorate, NASA Ames Research Center, for sparking his interest in the subject and for the insightful technical discussions during the course of this study. The interest of Jerry Miao and James Wang at Sikorsky Aircraft is also appreciated.

References

[1]Chopra, I., "Perspectives in Aeromechanical Stability of Helicopter Rotors," *Vertica*, Vol. 14, No. 4, 1990, pp. 457–508.

[2]Ormiston, R. A., "The Challenge of the Damperless Rotor," *Proceedings of the 22nd European Rotorcraft Forum* (Brighton, England, UK), 1996, pp. 27.1–27.14.

[3]Gandhi, F., "Concepts for Damperless Aeromechanically Stable Rotors," *Proceedings of the Innovation in Rotorcraft Technology Conference*, Royal Aeronautical Society, London, 1997, pp. 14.1–14.31.

[4]Young, M. I., and Bailey, D. J., "Stability and Control of Hingeless Rotor Helicopter Ground Resonance," *Journal of Aircraft*, Vol. 11, No. 6, 1974, pp. 333–339.

[5]Straub, F. K., and Warmbrodt, W., "The Use of Active Controls to Augment Rotor/Fuselage Stability," *Journal of the American Helicopter Society*, Vol. 30, No. 3, 1985, pp. 13–22.

[6]Straub, F. K., "Optimal Control of Helicopter Aeromechanical Stability," *Vertica*, Vol. 11, No. 3, 1987, pp. 425–435.

[7]Weller, W. H., "Fuselage State Feedback for Aeromechanical Stability Augmentation of a Bearingless Rotor," *Journal of the American Helicopter Society*, Vol. 41, No. 2, 1996, pp. 85–93.

[8]Gandhi, F., and Weller, W. H., "Active Aeromechanical Stability Augmentation Using Fuselage State Feedback," *Proceedings of the 53rd Annual Forum of the American Helicopter Society* (Virginia Beach, VA), 1997, pp. 1350–1362.

[9]Ormiston, R. A., "Techniques for Improving the Stability of Soft Inplane Hingeless Rotors," NASA TN X-62390, Oct. 1974.

[10]Bousman, W. G., Sharpe, D. L., and Ormiston, R. A., "An Experimental Study of Techniques for Increasing the Lead-Lag Damping of Soft Inplane Hingeless Rotors," *Proceedings of the 32nd Annual*

National V/STOL Forum of the American Helicopter Society (Washington, DC), 1976, pp. 1035.1–1035.12.

[11]Bousman, W. G., "The Effects of Structural Flap-Lag and Pitch-Lag Coupling on Soft Inplane Hingeless Rotor Stability in Hover," NASA TP 3002, May 1990.

[12]Ormiston, R. A., "Aeromechanical Stability of Soft Inplane Hingeless Rotor Helicopters," *Proceedings of the 3rd European Rotorcraft and Powered Lift Aircraft Forum* (Aix-en-Provence, France), 1977, pp. 25.1–25.22.

[13]Bousman, W. G., "An Experimental Investigation of the Effects of Aeroelastic Couplings on Aeromechanical Stability of a Hingeless Rotor Helicopter," *Journal of the American Helicopter Society*, Vol. 26, No. 1, 1981, pp. 46–54.

[14]Ormiston, R. A., "Investigations of Hingeless Rotor Stability," *Vertica*, Vol. 7, No. 2, 1983, pp. 143–181.

[15]King, S. P., "The Effect of Pitch-Flap and Pitch-Lag Coupling on Air Resonance," Dynamics Dept., Westland Helicopters, Ltd., Yeovil, Rept. GEN/DYN/RES/005R, July 1971.

[16]Nagabhushanam, J., and Gaonkar, G. H., "Rotorcraft Air Resonance in Forward Flight with Various Dynamic Inflow Models and Aeroelastic Couplings," *Proceedings of the 9th European Rotorcraft Forum* (Stresa, Italy), 1983, pp. 52.1–52.24.

[17]Milgram, J. H., and Chopra, I., "Air Resonance of Hingeless Rotor Helicopters in Trimmed Forward Flight," *Journal of the American Helicopter Society*, Vol. 39, No. 4, 1994, pp. 46–58.

[18]Zotto, M. D., and Loewy, R. G., "Influence of Pitch-Lag Coupling on Damping Requirements to Stabilize Ground/Air Resonance," *Journal of the American Helicopter Society*, Vol. 37, No. 4, 1992, pp. 68–71.

[19]Venkatesan, C., "Influence of Aeroelastic Couplings on Coupled Rotor/Body Dynamics," 6th International Workshop on Dynamics and Aeroelastic Stability Modeling of Rotorcraft Systems, Los Angeles, CA, Nov. 1995.

[20]Ormiston, R. A., and Hodges, D. H., "Linear Flap-Lag Dynamics of Hingeless Helicopter Rotor Blades in Hover," *Journal of the American Helicopter Society*, Vol. 17, No. 2, 1972, pp. 2–15.

[21]Peters, D. A., and HaQuang, N., "Dynamic Inflow for Practical Applications," *Journal of the American Helicopter Society*, Vol. 33, No. 4, 1988, pp. 64–68.